chelate (λ_{max} = 340 nm; ϵ not reported).[44] The shifts on deprotonation (in each case to lower energy) are rather similar in the three cases (25, 61, and 20 nm, respectively), a comparison that also suggests similar structures of the parent species.

Though the case we have made for oxygen protonation of the N-bound isomer of urea seems to us to be strong, the point cannot be taken as settled. When arguments of the type we have used are extended to the urea complex of $[(NH_3)_5Rh]^{3+}$, inconsistencies appear. Because Ru(III) is paramagnetic, the issue is not easily settled in solution by NMR evidence, nor, owing to rather rapid isomerization in the solid, does solid-state structure determination by X-ray diffraction seem feasible.

Acknowledgment. Support of this work by National Institutes of Health Grant GM13638-19 and National Science Foundation Grant CHE82-11275 are gratefully acknowledged.

Registry No. $[Ru(NH_3)_5OC(NH_2)_2]^{3+}$, 97352-84-6; $[Ru(NH_3)_5NH_2CONH_2]^{3+}$, 97352-85-7; $[Ru(NH_3)_5OP(OCH_3)_3]^{3+}$, 97352-86-8; $[Ru(NH_3)_5OP(OC_2H_5)_3]^{3+}$, 97352-87-9; $[Ru(NH_3)_5OC(CH_3)N(CH_3)_2]^{3+}$, 97352-88-0; $[Ru(NH_3)_5OCHNH_2]^{3+}$, 97352-94-8; $[Ru(NH_3)_5OCHN(CH_3)_2]^{3+}$, 97352-89-1; $[Ru(NH_3)_5NHCONH_2](PF_6)_2$, 97352-91-5; $[Ru(NH_3)_5O_3SCF_3](CF_3SO_3)_2$, 84278-98-8; $[Ru(NH_3)_5OC(NH_2)_2](PF_6)_3$, 97352-92-6; $[Ru(NH_3)_5OC(NH_2)_2](BF_4)_3$, 97352-93-7; $[Ru(NH_3)_5OCHNH_2](PF_6)_3$, 97352-95-9; $[Ru(NH_3)_5OCHN(CH_3)_2]_2(S_2O_6)_3$, 97352-96-0; $[Ru(NH_3)_5OC(CH_3)N(CH_3)_2]_2(S_2O_6)_3$, 97352-97-1; $[Ru(NH_3)_5OP(OCH_3)_3]_2(S_2O_6)_3$, 97414-11-4; $[Ru(NH_3)_5OP(OC_2H_5)_3]_2(S_2O_6)_3$, 97352-98-2.

Supplementary Material Available: Tables of rate constants for isomerization of $[(NH_3)_5RuNH_2CONH_2]^{3+}$ (Table II), acid hydrolysis of $[(NH_3)_5ML]^{n+}$ (Table III), and linkage isomerization and aquation of $[(NH_3)_5RuNH_2CONH_2]^{3+}$ (Table IV) and equilibrium and rate constants for linkage isomerism of $[(NH_3)_5ML]^{3+}$ (Table V) (4 pages). Ordering information is given on any current masthead page.

(44) Ilan, Y.; Taube, H. *Inorg. Chem.* **1983**, *22*, 1657.

Contribution from the Department of Chemistry, University of Minnesota, Minneapolis, Minnesota 55455

N–O Bond Cleavage of Cluster-Coordinated Nitric Oxide Ligands Using Molecular Hydrogen

JOANNE A. SMIEJA, ROBERT E. STEVENS, DOUGLAS E. FJARE, and WAYNE L. GLADFELTER*[1]

Received January 23, 1985

The reaction of several clusters containing nitric oxide ligands with molecular hydrogen has been studied. For $HRu_3(CO)_{10}(NO)$ the products are $H_2Ru_3(NH)(CO)_9$, $HRu_3(NH_2)(CO)_{10}$, $H_4Ru_4(CO)_{12}$, trace amounts of $H_3Ru_4(NH_2)(CO)_{12}$, and a hexane-insoluble, THF-soluble precipitate. The compounds have been characterized by spectroscopy (including ^{15}N NMR) and for $HRu_3(NH_2)(CO)_{10}$ by a single-crystal X-ray crystallographic analysis (monoclinic crystal system, $P2_1/a$ space group, a = 11.778 (3) Å, b = 11.928 (3) Å, c = 12.010 (4) Å, β = 98.54 (2)°, Z = 4). A system was built that allowed the reactions to be followed directly by high-pressure liquid chromatography. A kinetic analysis of the disappearance of $HRu_3(CO)_{10}(NO)$ revealed that the reaction is first order in cluster concentration and is inhibited by CO. The rate also depends on the pressure of H_2, exhibiting a saturation effect above 1400 psig. The reduction of $Ru_3(NOCH_3)(CO)_{10}$ yields a product distribution similar to that found for $HRu_3(CO)_{10}(NO)$ with the important exception that no hexane-insoluble species is formed. Methanol is isolated from this reaction. The major product resulting from the reduction of $Ru_3(NOH)(CO)_{10}$ is the same hexane-insoluble product as found for $HRu_3(CO)_{10}(NO)$. A discussion of the mechanism of these reactions based upon the observations is presented.

Introduction

The need to remove toxic NO_x pollutants from the atmosphere has led to the development of several catalytic methods to reduce nitric oxide.[2,3] The reducing agent is either CO or H_2, and the products are shown in eq 1 and 2. The reduction of NO with

$$2NO + 2CO \rightleftharpoons N_2 + 2CO_2 \quad (1)$$

$$2NO + 5H_2 \rightleftharpoons 2NH_3 + 2H_2O \quad (2)$$

CO can be effected with use of either heterogeneous or homogeneous catalysts (the latter catalysts produce N_2O instead of N_2), while only the heterogeneous systems have been used for eq 2.

Recent interest in clusters containing the NO ligand has centered around the reduction of the N–O bond. In several examples cluster-coordinated NO has been reduced with CO to produce CO_2 and a nitrido cluster.[4,5] This reaction bears a striking similarity to eq 1 in which surface-absorbed nitrogen atoms have been postulated as intermediates. Alternatively, the triply bridging nitrosyl ligand in $(\eta^5\text{-}C_5H_4Me)_3Mn_3(NO)_4$ can be reduced to a μ_3-NH ligand with use of protons.[6] The electrons required for this conversion apparently are derived by sacrificially oxidizing some of the cluster species present. The use of protons and electrons to reduce a coordinated NO on the mononuclear complex $[Ru(trpy)(bpy)(NO)]^{3+}$ has been accomplished by electrochemical means.[7]

In a preliminary communication of this work we reported the first use of molecular hydrogen to reduce the coordinated NO of $HRu_3(CO)_{10}(NO)$.[8] Recently an independent study of this same reaction was also reported that involved the direct observation of the reaction solution by using a high-pressure infrared cell.[9] While the final products observed in both of these studies are similar, some differences in the proposed steps of the reaction exist. In this study we present the details of our work with $HRu_3(CO)_{10}(NO)$ and the closely related cluster $Ru_3(CO)_{10}(NOCH_3)$. The combination of these results has allowed us to address some

(1) Fellow of the Alfred P. Sloan Foundation (1983–1985).
(2) Eisenberg, R.; Hendriksen, D. E. *Adv. Catal.* **1979**, *28*, 79.
(3) Savatsky, B. J.; Bell, A. T. *ACS Symp. Ser.* **1982**, *no. 178*, 105.
(4) Fjare, D. E.; Gladfelter, W. L. *J. Am. Chem. Soc.* **1984**, *106*, 4799.
(5) Collins, M. A.; Johnson, B. F. G.; Lewis, J.; Mace, J. M.; Morris, J.; McPartlin, M.; Nelson, W. J. H.; Puga, J.; Raithby, P. R. *J. Chem. Soc., Chem. Commun.* **1983**, 689.
(6) Legzdins, P.; Nurse, C. R.; Rettig, S. J. *J. Am. Chem. Soc.* **1983**, *105*, 3727.
(7) Murphy, W. R., Jr.; Takeuchi, K. J.; Meyer, T. J. *J. Am. Chem. Soc.* **1982**, *104*, 5817.
(8) Gladfelter, W. L. In "Organometallic Compounds: Synthesis, Structure, and Theory"; Shapiro, B. L., Ed.; Texas A & M University Press: College Station, TX, 1983; p 281.
(9) Johnson, B. F. G.; Lewis, J.; Mace, J. M. *J. Chem. Soc., Chem. Commun.* **1984**, 186.

0020-1669/85/1324-3206$01.50/0

Table I. Spectroscopic Properties of New Compounds

compd	color	ν_{CO}, cm^{-1} (hexane)	ν_{N-H} or ν_{N-O}, cm^{-1}	^1H NMR, ppm ($CDCl_3$)	^{15}N NMR, ppm (CH_2Cl_2)
$H_2Ru_3(NH)(CO)_9$	yellow	2116 m, 2080 s, 2056 vs, 2046 s, 2012 s, 2002 s, 1989 m, 1975 vw, 1970 vw	3362 vw, 3353 vw (^{15}N)	6.36 (1 H), −17.49 (2 H)	82.5 ($J_{^{15}N-^1H}$ = 77.5 Hz)
$HRu_3(NH_2)(CO)_{10}$	orange	2103 w, 2067 s, 2052 s, 2026 s, 2012 s, 2005 s, 1996 w, 1987 w, 1969 vw	3405 vw, 3345 vw, 3396 vw (^{15}N), 3338 vw (^{15}N)	2.74 (1 H, br), 1.84 (1 H, br), −13.88 (1 H, J_{HH} = 2.5, 1.0 Hz)	−33.5 ($J_{^{15}N-^1H}$ = 72.7, 70.8, 2.5 Hz)
$H_2Ru_3(NOCH_3)(CO)_9$	yellow	2115 w, 2078 m, 2057 vs, 2049 s, 2038 w, 2009 vs, 2001 s, 1988 vw	929 m, 902 m (^{15}N)	3.48 (3 H, s, $J_{^{15}N-^1H}$ = 3.9 Hz), −17.8 (2 H, s, $J_{^{15}N-^1H}$ = 1.8 Hz)	301.0
$H_3Ru_4(NH_2)(CO)_{12}$	orange	2103 vw, 2074 s, 2058 vs, 2020 sh, 2015 s, 2000 w	3367 vw, 3311 vw, 3358 vw (^{15}N), 3304 vw (^{15}N)	−1.08 (2 H, s), −16.09 (3 H, s)	

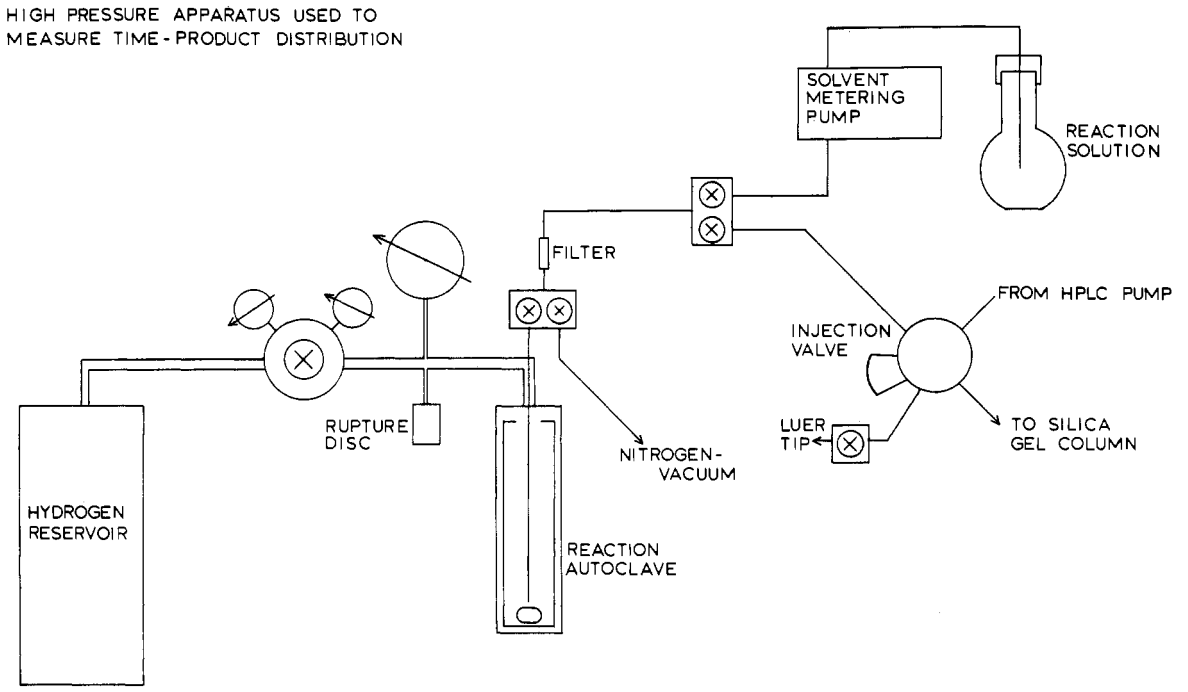

Figure 1. Diagram of the apparatus used to monitor the high-pressure reactions with HPLC.

of the important aspects of the reduction of NO with molecular hydrogen.

Experimental Section

$HRu_3(CO)_{10}(NO)$,[10] $Ru_3(NOCH_3)(CO)_{10}$,[11] $Ru_3(NOH)(CO)_{10}$,[11] $Ru_3(NPh)(CO)_{10}$,[12] and $H_2Ru_3(NPh)(CO)_9$[12] were prepared with use of literature methods. Tetrahydrofuran (THF) and diethyl ether were distilled from sodium–benzophenone ketyl, CH_2Cl_2 was distilled from P_2O_5, and hexane was distilled from sodium metal prior to use. Other reagents, purchased from commercial sources, were used as received. Hydrogen was the chemically pure grade. Infrared spectra were recorded on a Beckman Model 4250 spectrophotometer or a Mattson Cygnus 25 FTIR equipped with a HgCdTe detector. The NMR data were recorded on a Nicolet NTCFT-1180 300-MHz spectrometer. The electron impact mass spectral data were obtained with the solids probe of an AEI-MS30 instrument. The samples for the ^{15}N NMR experiments were prepared from $Na^{15}NO_2$ (95% enriched) obtained from Merck Sharp and Dohme. A list of the spectroscopic data for the new compounds presented here is given in Table I.

Procedure for Monitoring High-Pressure Reactions. In reference to Figure 1, a 35-mL glass liner containing a stir bar was placed inside a 71-mL Parr high-pressure reaction autoclave. The autoclave was sealed, and a 0.01 in. inner diameter dip tube connected to a Scientific Systems two-step, two-way valve was inserted vertically through a T-tube into the pressure vessel. The autoclave and the gas reservoir were repeatedly pressurized and vented with N_2 and then pressurized and vented three times with H_2. Both were brought to the desired pressure of H_2. The reservoir was further pressurized to 3000 psig. Constant pressure was maintained with use of the regulator attached to the reservoir.

The reaction autoclave was heated to the desired temperature with use of either a heating jacket in which the temperature was monitored with a thermometer placed between the heating jacket and the autoclave or an aluminum block containing heating rods controlled by a proportional temperature controller. After the desired reaction temperature had been reached, an additional 30 min was allowed for the autoclave to equilibrate with the surroundings.

At this point a solution containing the cluster to be studied and triphenylmethane (internal standard) was deoxygenated and then injected into the autoclave with use of a Milton Roy minipump. This injection technique usually required about 1 min and gave an accurate initial time for the kinetic experiments.

The high-pressure reaction was monitored by periodically analyzing samples on a HPLC. The tubing between the reaction autoclave and HPLC was flushed with hexane and evacuated to prepare for each new injection. The total volume of each sample removed was 0.4 mL.

General Procedure for Preparative Reactions. In a typical experiment, a measured amount of cluster was dissolved in heptane and placed in a glass liner. The liner was placed inside a rocking autoclave that was pressurized with N_2 and vented. This procedure was repeated several times with N_2 followed by three times with H_2. The autoclave was pressurized to the desired level with H_2. Rocking and heating of the autoclave was begun, and the temperature was monitored with a thermocouple inserted in the autoclave. The reported reaction times correspond to the amount of time the autoclave was at the reaction temperature. After the autoclave was cooled, it was depressurized, and the reaction solution was taken out of the bomb, filtered, and chromatographed on silica gel.

Reduction of $HRu_3(CO)_{10}(NO)$. With use of the above procedure $HRu_3(CO)_{10}(NO)$ was dissolved in heptane and reacted with hydrogen

(10) Stevens, R. E.; Gladfelter, W. L. *Inorg. Chem.* **1983**, *22*, 2034.
(11) Stevens, R. E.; Gladfelter, W. L. *J. Am. Chem. Soc.* **1982**, *104*, 6454.
(12) Sappa, E.; Milone, L. *J. Organomet. Chem.* **1973**, *61*, 383.

Table II. Product Yields in the Batch Reductions of $HRu_3(CO)_{10}(NO)$

conditions	% product			
	$HRu_3(NO)(CO)_{10}$	$H_4Ru_4(CO)_{12}$	$H_2Ru_3(NH)(CO)_9$	$HRu_3(NH_2)(CO)_{10}$
1000 psig H_2, 75 °C, 2 h	17	4	8	14
2000 psig H_2, 75 °C, 2 h	14	8	10	34
3000 psig H_2, 75 °C, 2 h	10	6	8	28
~15 psig H_2, 68 °C, 3.5 h	64	trace		trace
~15 psig H_2, 68 °C, 8 h	...	trace	trace	
2000 psig H_2, 75 °C, 1 h	18	8	12	15
2000 psig H_2, 75 °C, 4 h	5	13	5	36
2000 psig H_2, 75 °C, 8 h	~1	21	~1	34

at 75 °C. After completion of the reaction a red-brown precipitate was present in the yellow solution. This was removed by filtration, and the clear yellow solution was chromatographed. The first band to elute was $H_4Ru_4(CO)_{12}$.[13] This was followed by a brown band that contained unreacted $HRu_3(CO)_{10}(NO)$. The third band was yellow and contained $H_2Ru_3(NH)(CO)_9$,[14] while the fourth band was orange and contained $HRu_3(NH_2)(CO)_{10}$. In large-scale reactions a fifth band appeared and was found to be $H_3Ru_4(NH_2)(CO)_{12}$.

The conditions found to give the optimum yield of $H_2Ru_3(NH)(CO)_9$ were as follows: 2000 psig of H_2, 75 °C, 1-h reaction time. Under these conditions, 74.8 mg (0.122 mmol) of $HRu_3(CO)_{10}(NO)$ dissolved in 10 mL of heptane gave 8.1 mg (0.014 mmol) of $H_2Ru_3(NH)(CO)_9$ (12% yield) as yellow crystals. Anal. Calcd for $H_2Ru_3(NH)(CO)_9$: C, 18.89; H, 0.53; N, 2.45. Found: C, 18.86; H, 0.57; N, 2.39. Mass spectral data for $H_2Ru_3(NH)(CO)_9$ have been reported.[14]

The conditions used to give the optimum yield of $HRu_3(NH_2)(CO)_{10}$ were as follows: 2000 psig of H_2, 75 °C, 4-h reaction time. With use of 150.4 mg (0.245 mmol) of $HRu_3(CO)_{10}(NO)$ dissolved in 20 mL of heptane, orange crystals of $HRu_3(NH_2)(CO)_{10}$ (52.5 mg, 0.087 mmol) in 36% yield were obtained after chromatography. Anal. Calcd for $HRu_3(NH_2)(CO)_{10}$: C, 20.01; H, 0.50; N, 2.33. Found: C, 20.08; H, 0.50; N, 2.34. The mass spectrum revealed a parent ion at $m/z = 601$ (^{102}Ru). A summary of yields for this reaction as a function of conditions is given in Table II.

The red-brown precipitate is completely soluble in THF or CH_2Cl_2. The infrared spectrum in the carbonyl region has absorptions at 2110 w, 2080 w (sh), 2045 vs, 2002 s, and 1950 w (sh) cm^{-1}, and no peaks were observed in the ν_{N-H} region. A complete elemental analysis (except for oxygen, which was obtained by difference) gave the following results. Anal. Found: C, 21.27; H, 1.89; N, 2.83; Ru, 45.59. The ^1H NMR spectrum revealed absorptions in the metal hydride region at −16.28, −16.36, −17.2, and −21.1 ppm.

A test was performed to determine whether the precipitate had any effect on the reaction. Immediately following a typical reaction the solution in the glass liner was decanted from the solid, which was then washed with deoxygenated heptane. A fresh heptane solution of $HRu_3(CO)_{10}(NO)$ was added to the solid, and the liner was returned to the autoclave. The reaction was conducted in the usual manner and monitored with HPLC. There was no difference between this run and the prior run in which precipitate was initially generated.

In order to examine the effect of CO on the rate of this reaction, the apparatus was prepared in the usual way and charged with 500 psig of CO and 1500 psig of H_2. The reaction solution was added, and the reaction was begun. Even after 14 h no appreciable decrease in starting material had occurred.

Reduction of $Ru_3(NOH)(CO)_{10}$. With use of the procedure described for monitoring reactions, the system was pressurized to 2100 psig of H_2 and heated to 55 °C. When the temperature stabilized, a clear lemon yellow hexane solution of $Ru_3(NOH)(CO)_{10}$ (21 mL) was pumped into the autoclave with a HPLC pump. The reaction was stirred and monitored by infrared spectroscopy ($Ru_3(NOH)(CO)_{10}$ could not be chromatographed). After 80 min all of the $Ru_3(NOH)(CO)_{10}$ had been consumed as shown by the disappearance of the bridging carbonyl band at 1744 cm^{-1}. The reaction mixture was allowed to cool to room temperature, the pressure was released, and the glass liner was removed to reveal a very cloudy yellow solution. The mixture was quickly transferred to a Schlenk tube and placed under nitrogen. The solvent was removed under vacuum, and the residue was extracted and filtered with hexane to give a clear yellow solution and a reddish solid. The hexane solution was concentrated and chromatographed to give four yellow bands. Band 1 (0.5 mg) was identified by infrared spectroscopy to be a mixture of $Ru_3(CO)_{12}$ and $H_4Ru_4(CO)_{12}$. Bands 2–4 were identified by infrared spectroscopy as $HRu_3(CO)_{10}(NO)$ (0.5 mg), $H_2Ru_3(NH)(CO)_9$ (0.1 mg), and $HRu_3(NH_2)(CO)_{10}$ (1.0 mg). The red hexane-insoluble solid (5.6 mg) was completely dissolved in THF to give a pale orange solution. An infrared spectrum of this solid was very similar to that of the solid produced in the reduction of $HRu_3(CO)_{10}(NO)$.

Reaction of $H_2Ru_3(NH)(CO)_9$ with CO. $H_2Ru_3(NH)(CO)_9$ (23.6 mg, 0.041 mmol) was dissolved in 10 mL of hexane and placed under 50 psig of CO. The reaction vessel was heated to 95 °C. After 1.5 h heating was stopped, and the reaction mixture was chromatographed. The first band was yellow and contained unreacted $H_2Ru_3(NH)(CO)_9$ (10.3 mg, 0.018 mmol) corresponding to 44% of the starting material. The second band was orange and contained $HRu_3(NH_2)(CO)_{10}$ (13.2 mg, 0.022 mmol) to give a 54% conversion.

Attempted Conversion of $HRu_3(NH_2)(CO)_{10}$ to $H_2Ru_3(NH)(CO)_9$. $HRu_3(NH_2)(CO)_{10}$ (31.6 mg, 0.053 mmol) was placed in a three-neck round-bottom flask equipped with condenser, gas inlet, and septum. The flask was degassed and filled with N_2, and freshly distilled decalin (15 mL) was added. The solution was brought to reflux (160 °C) for 5 h, during which time it turned from orange to dark brown. The reaction was monitored by infrared spectroscopy, and no peaks corresponding to the desired product, $H_2Ru_3(NH)(CO)_9$, appeared as the peaks corresponding to $HRu_3(NH_2)(CO)_{10}$ slowly disappeared. After completion the solution was cooled, filtered, and chromatographed. The major hexane-soluble product was a trace amount of an unidentified pink ruthenium carbonyl species. Several other attempts at converting $HRu_3(NH_2)(CO)_{10}$ into $H_2Ru_3(NH)(CO)_9$ using other thermal conditions, photolysis, and oxidative decarbonylation with Me_3NO were all unsuccessful.

Reaction of $HRu_3(NH_2)(CO)_{10}$ with H_2. $HRu_3(NH_2)(CO)_{10}$ (25.6 mg, 0.043 mmol) was dissolved in 20 mL of heptane and placed in the autoclave. With use of the procedure for preparative-scale reactions the autoclave was pressurized to 2000 psig of H_2 and heated to 70 °C for 16 h. The system was depressurized, and the reaction solution was chromatographed. The first band was yellow and contained $H_4Ru_4(CO)_{12}$ characterized by infrared spectroscopy. The solvent was removed to give a yellow powder (3.4 mg, 0.0046 mmol) of $H_4Ru_4(CO)_{12}$ in 14% yield. The second band was orange and contained unreacted $HRu_3(NH_2)(CO)_{10}$ (21.6 mg, 0.036 mmol) corresponding to 84% of the starting material.

Preparation of $H_2Ru_3(NOCH_3)(CO)_9$. $Ru_3(NOCH_3)(CO)_{10}$ (95.0 mg, 0.151 mmol) was dissolved in hexane (15 mL), and the solution was placed in a Griffin–Worden pressure vessel. The vessel was evacuated and filled with H_2 four times to remove oxygen. The hydrogen pressure was maintained at 35 psig, and the vessel was immersed in a water bath maintained at 60 °C for 5 h. The solution was allowed to cool to room temperature under H_2, after which the hydrogen pressure was released and the yellow solution was chromatographed, giving one yellow band. The solvent was removed on a rotary evaporator to give $H_2Ru_3(NOCH_3)(CO)_9$ (78.8 mg, 0.132 mmol) in 88% yield. Mass spectrum: $m/z = 604$ (parent), followed by loss of OCH_3 and nine peaks each corresponding to a loss of carbon monoxide. Anal. Calcd for $Ru_3O_{10}NC_{10}H_5$: C, 19.94; H, 0.84; N, 2.30. Found: C, 20.03; H, 0.90; N, 2.34.

Detection of Methanol. $Ru_3(NOCH_3)(CO)_{10}$ (56.8 mg, 0.090 mmol) was dissolved in C_6D_6 (4.5 mL), and the bright yellow solution was bubbled with N_2 for 5 min. The solution was placed in a glass liner and sealed in a stainless steel autoclave. The apparatus was purged with N_2, pressurized to 2550 psig with H_2, and heated to 80 °C for 20 h. The bomb was allowed to cool to room temperature, and the pressure was carefully released. The glass liner was removed from the autoclave, revealing a clear orange solution and a yellow solid. The mixture was quickly transferred to a flame-dried Schlenk tube. A portion of the orange solution was placed in an NMR tube, and a proton spectrum showed a doublet at 2.98 ppm ($J = 5.0$ Hz) corresponding to the methyl group of CH_3OH. The orange solution was returned to the Schlenk tube, and the mixture was vacuum distilled into another flame-dried Schlenk

(13) (a) Kaesz, H. D.; Knox, S. A. R.; Koepke, J. W.; Saillant, R. B. *J. Chem. Soc., Chem. Commun.* **1971**, 477. (b) Knox, S. A. R.; Koepke, J. W.; Andrews, M. A.; Kaesz, H. D. *J. Am. Chem. Soc.* **1975**, *97*, 3942.
(14) Fjare, D. E.; Keyes, D. G.; Gladfelter, W. L. *J. Organomet. Chem.* **1983**, *250*, 383.

Table III

Crystal Parameters	
cryst syst: monoclinic	V = 1669 (1) Å^3
space group: $P2_1/a$	Z = 4
a = 11.778 (3) Å	calcd density: 2.39 g cm^{-3}
b = 11.928 (3) Å	temp: 23 °C
c = 12.010 (4) Å	abs coeff: 26.65 cm^{-1}
β = 98.54 (2)°	

Measurement of Intensity Data
diffractometer: Enraf-Nonius CAD 4
radiation: Mo Kα (λ = 0.71073 Å)
monochromator: graphite cryst
scan type: ω–2θ
scan speed: 1.11–6.67°/min
scan range: $0° \leq 2\theta \leq 60°$
reflcns measd: $h,+k,+l$
check reflcns: {800}, {008}, {054}
reflcns collected: 4862 unique reflcns; 4121 with $I > 2\sigma(I)$
p = 0.04
R = 0.024
R_w = 0.039
error in observn of unit wt: 1.427

tube. A proton NMR spectrum of the clear colorless solution again showed the methanol doublet. Separation of the residue from the distillation by liquid chromatography gave $H_4Ru_4(CO)_{12}$ (35.2 mg, 0.047 mmol) and $HRu_3(NH_2)(CO)_{10}$ (6.3 mg, 0.010 mmol), which corresponds to 81% recovery of the ruthenium.

Carbonylation of $H_2Ru_3(NPh)(CO)_9$. A hexane solution of $H_2Ru_3(NPh)(CO)_9$ was placed under an atmosphere of 50 psig of CO. After 2 h at 95 °C infrared spectroscopy indicated that no reaction had occurred. The temperature was raised to 110 °C, and after 5 h absorbances due to $HRu_3(NHPh)(CO)_{10}$ and a lesser amount of $Ru_3(NPh)(CO)_{10}$ were clearly observable. The reaction was continued at 100 °C for an additional 15 h, and a HPLC analysis of the mixture revealed approximately 60% of the $H_2Ru_3(NPh)(CO)_9$ had remained unchanged, while 30% of $HRu_3(NHPh)(CO)_{10}$ had formed. Approximately 10% of $Ru_3(NPh)(CO)_{10}$ was present. The compounds were then separated on a preparative silica gel column and characterized by infrared spectroscopy to confirm their identity.

Collection and Reduction of the X-ray Data. Orange crystals of $HRu_3(NH_2)(CO)_{10}$ were grown by slow cooling of a hexane solution to −25 °C. One crystal of dimensions 0.26 × 0.37 × 0.31 mm was mounted in air on a glass fiber. The crystal was found to be monoclinic by the Enraf-Nonius CAD4-SDP peak search, centering, and indexing programs and by a Delauney reduction calculation.[15] A summary of the crystal data is presented in Table III. Background counts were measured at both ends of the scan range with the use of a ω–2θ scan, equal at each side to one-fourth of the scan range of the peak. In this manner, the total duration of measuring background is equal to half of the time required for the peak scan. The three check reflections showed no change in intensity during data collection. A total of 4862 unique reflections were measured, of which 4121 had $I > 2\sigma(I)$ and were used in the structural determination. The space group $P2_1/a$ was determined from the observed systematic absences of $h0l$, $h = 2n + 1$ absent, and $0k0$, $k = 2n + 1$ absent. Successful refinement of the structure verified the choice of this space group. ψ scans were run on reflections {212}, {426}, {639}, and {8,5,12} and showed the need for an absorption correction with transmission factors of minimum 85.59, maximum 99.90, and average 91.78. The data were corrected for Lorentz, polarization, and background effects, and an empirical absorption correction was applied.[16]

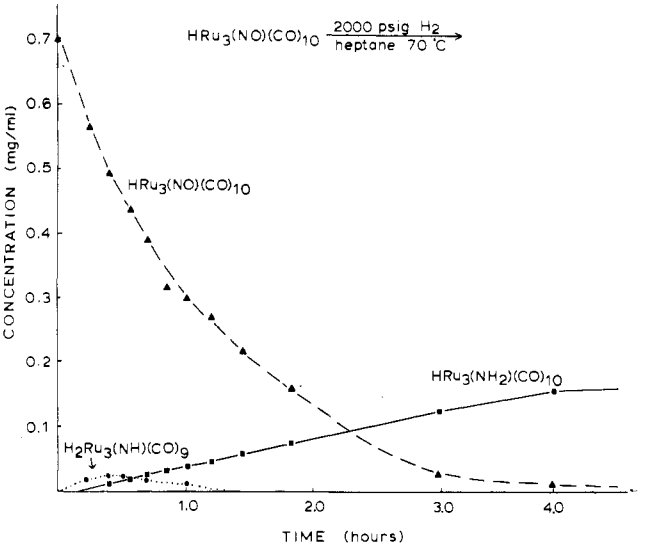

Figure 2. Graph showing the product distribution as a function of time for the reduction of $HRu_3(CO)_{10}(NO)$.

Solution and Refinement of the Structure. The structure was solved by conventional heavy-atom techniques. The positions of the three ruthenium atoms were determined by a Patterson synthesis. Isotropic refinement of the ruthenium atoms converged at R = 0.217. A difference Fourier synthesis then revealed the positions of all of the remaining non-hydrogen atoms.[17] Isotropic refinement of this model converged at R = 0.066. At this point the thermal parameters of all atoms were made anisotropic, and further refinement converged at R = 0.030. A difference Fourier synthesis then revealed the positions of H1 and H2. The position of H3 was idealized, and the final refinement was carried out with anisotropic temperature factors for all non-hydrogen atoms and isotropic temperature factors for the hydrogen atoms which were included in the refinement. This refinement converged to R = 0.025 and R_w = 0.039. The volume of the atomic scattering factors was taken from the usual tabulation, and the effects of anomalous dispersion were included for the non-hydrogen atoms.[18] The hydrogen atom scattering factors were taken from Cromer and Ibers' list.[19] A final difference map showed no unusual features. A list of the final positional parameters is given in Table IV, and Tables V and VI report the distances and selected angles, respectively.

Results

The initial studies of the high-pressure reactions reported in this paper were all conducted as batch processes. The basic inaccuracy of this procedure as well as the prohibitive time requirements of successive batch runs prompted us to design a system that would allow us to continuously monitor the reaction without perturbing the reaction. The system shown in Figure 1 allowed us to directly remove a sample and analyze it with a HPLC. Samples could also be removed and then examined by infrared spectroscopy under ambient conditions. The small sample size required for injection (10 μL) into the HPLC allowed us to reduce the reaction solution volume (~10–20 mL) and ultimately the size of the entire apparatus. Two distinct advantages were obtained from this: the quantity of cluster required was greatly reduced, and the operational safety was improved. The addition of the second HPLC pump to deliver the solution to an autoclave that was preequilibrated at the correct temperature and pressure allowed a much more accurate definition of the start of the experiment. For synthetic purposes most of the reactions were run with use of a normal rocking autoclave.

(15) All calculations were carried out on PDP 8A and 11/34 computers using the Enraf-Nonius CAD 4-SDP programs. This crystallographic computing package is described in: Frenz, B. A. In "Computing in Crystallography"; Schenk, H., Olthof-Hazekamp, R., van Koningsveld, H., Bassi, G. C., Eds.; Delft University Press: Delft, Holland, 1978; pp 64–71. See also: "CAD 4 and SDP User's Manual"; Enraf-Nonius: Delft, Holland, 1978.

(16) The intensity data were processed as described: "CAD 4 and SDP User's Manual"; Enraf-Nonius: Delft, Holland, 1978. The net intensity $I = (K/\text{NPI})(C - 2B)$, where K = 20.1166 × (attenuator factor), NPI = ratio of fastest possible scan rate for the measurement, C = total count, and B = total background count. The standard deviation in the net intensity is given by $\sigma^2(I) = (K/\text{NPI})^2[C + 4B + (pI)^2]$, where p is a factor used to downweight intense reflections. The observed structure factor amplitude F_o is given by $F_3 = (I/Lp)^{1/2}$, where Lp = Lorentz and polarization factors. The $\sigma(I)$'s were converted to the estimated errors in the relative structure factors $\sigma(R_o)$ by $\sigma(R_o) = 1/2(\sigma(I)/I)F_o$.

(17) The function minimized was $\sum w(|F_o| - |F_c|)^2$, where $w = 1/\sigma^2(F_o)$. The unweighted and weighted residuals are defined as $R = (\sum||F_o| - |F_c||)/\sum|F_o|$ and $R_w = [(\sum w(|F_o| - |F_c|)^2/(\sum w|F_o|)^2]^{1/2}$. The error in an observation of unit weight is $[\sum w(|F_o| - |F_c|)^2/(\text{NO} - \text{NV})]^{1/2}$, where NO and NV are the number of observations and variables, respectively.

(18) Cromer, D. T.; Waber, J. T. "International Tables for X-ray Crystallography"; Kynoch Press: Birmingham, England, 1974; Vol. IV, Table 2.2A. Cromer, D. T. *Ibid.*, Table 2.3.1.

(19) Cromer, D. T.; Ibers, J. A. "International Tables for X-ray Crystallography"; Kynoch Press: Birmingham, England, 1974; Vol. IV.

Table IV. Positional Parameters for $HRu_3(NH_2)(CO)_{10}$

atom	x	y	z	atom	x	y	z
Ru1	0.16756 (2)	−0.02585 (2)	0.19416 (2)	C11	0.1109 (3)	−0.1414 (3)	0.0892 (3)
Ru2	0.40582 (2)	−0.05866 (2)	0.20276 (2)	C12	0.1839 (3)	0.0802 (3)	0.0762 (3)
Ru3	0.32908 (2)	0.10676 (2)	0.33540 (2)	C13	0.0268 (3)	0.0400 (3)	0.2290 (4)
				C14	0.1837 (3)	−0.1281 (3)	0.3213 (3)
O11	0.0775 (3)	−0.2079 (2)	0.0251 (3)	C21	0.3914 (3)	−0.2132 (3)	0.2412 (3)
O12	0.1930 (2)	0.1397 (2)	0.0043 (2)	C22	0.3791 (3)	−0.0922 (3)	0.0466 (3)
O13	−0.0541 (3)	0.0809 (3)	0.2462 (4)	C23	0.5713 (3)	−0.0715 (3)	0.2207 (3)
O14	0.1879 (3)	−0.1893 (2)	0.3932 (2)	C31	0.2553 (4)	0.0653 (3)	0.4605 (3)
O21	0.3904 (2)	−0.3046 (2)	0.2640 (3)	C32	0.4527 (3)	0.1810 (3)	0.4291 (3)
O22	0.3620 (3)	−0.1102 (3)	−0.0462 (2)	C33	0.2338 (3)	0.2349 (3)	0.3082 (39)
O23	0.6663 (2)	−0.0831 (3)	0.2260 (4)				
O31	0.2108 (3)	0.0414 (3)	0.5342 (3)	H1	0.410 (3)	−0.027 (3)	0.343 (3)
O32	0.5237 (3)	0.2271 (3)	0.4856 (3)	H2	0.483 (3)	0.139 (3)	0.206 (3)
O33	0.1783 (2)	0.3130 (2)	0.2913 (3)	H3	0.396 (3)	0.133 (3)	0.128 (3)
N	0.4111 (2)	0.1171 (2)	0.1918 (2)				

Table V. Bond Distances (Å) for $HRu_3(NH_2)(CO)_{10}$

Ru1–Ru2	2.820 (1)	Ru2–H1	1.72 (3)
Ru1–Ru3	2.836 (1)	Ru3–H1	1.86 (3)
Ru2–Ru3	2.770 (1)		
		N–H2	0.88 (3)
Ru2–N	2.102 (2)	N–H3	0.79 (4)
Ru3–N	2.101 (2)		
		C11–O11	1.135 (4)
Ru1–C11	1.919 (3)	C12–O12	1.136 (4)
Ru1–C12	1.930 (3)	C13–O13	1.116 (4)
Ru1–C13	1.935 (3)	C14–O14	1.126 (4)
Ru1–C14	1.941 (3)	C21–O21	1.125 (3)
Ru2–C21	1.914 (3)	C22–O22	1.124 (4)
Ru2–C22	1.897 (3)	C23–O23	1.120 (4)
Ru2–C23	1.935 (3)	C31–O31	1.130 (4)
Ru3–C31	1.909 (3)	C32–O32	1.137 (4)
Ru3–C32	1.919 (3)	C33–O33	1.139 (4)
Ru3–C33	1.896 (3)		

Table VI. Selected Bond Angles (deg) for $HRu_3(NH_2)(CO)_{10}$

Ru2–Ru1–Ru3	58.66 (1)	Ru2–Ru3–N	48.77 (6)
Ru2–Ru1–C11	99.89 (9)	Ru2–Ru3–C31	119.6 (1)
Ru2–Ru1–C12	84.88 (9)	Ru2–Ru3–C32	112.5 (1)
Ru2–Ru1–C13	158.1 (1)	Ru2–Ru3–H1	38 (1)
Ru2–Ru1–C14	84.46 (9)	N–Ru3–C31	168.3 (1)
Ru3–Ru1–C13	99.5 (1)	N–Ru3–H1	78 (1)
Ru3–Ru1–C14	84.34 (9)	C33–Ru3–H1	172 (1)
Ru3–Ru1–C11	158.58 (9)		
C12–Ru1–C14	168.6 (1)	Ru2–N–Ru3	82.47 (8)
		Ru2–N–H2	109 (2)
Ru1–Ru2–Ru3	60.95 (1)	Ru2–N–H3	108 (3)
Ru1–Ru2–C21	91.09 (8)	Ru3–N–H2	114 (2)
Ru1–Ru2–C22	88.56 (9)	Ru3–N–H3	139 (3)
Ru1–Ru2–C23	174.6 (1)	H2–N–H3	100 (3)
Ru1–Ru2–N	84.14 (7)		
Ru1–Ru2–H1	84 (1)	Ru1–C11–O11	178.3 (3)
Ru3–Ru2–N	48.76 (6)	Ru1–C12–O12	177.7 (3)
Ru3–Ru2–H1	41 (1)	Ru1–C13–O13	177.4 (4)
Ru3–Ru2–C21	119.13 (8)	Ru1–C14–O14	176.7 (3)
Ru3–Ru2–C22	134.27 (9)	Ru2–C21–O21	175.5 (3)
Ru3–Ru2–C23	113.7 (1)	Ru2–C22–O22	178.7 (3)
N–Ru2–C22	98.7 (1)	Ru2–C23–O23	176.0 (3)
N–Ru2–H1	81 (1)	Ru3–C31–O31	179.4 (4)
C22–Ru2–H1	172 (1)	Ru3–C32–O32	178.0 (3)
C21–Ru2–H1	88 (1)	Ru3–C33–O33	178.7 (3)
Ru1–Ru3–Ru2	60.39 (1)		
Ru1–Ru3–N	83.75 (7)		
Ru1–Ru3–C32	172.44 (9)		
Ru1–Ru3–H1	81 (1)		

$HRu_3(CO)_{10}(NO) + H_2$. The reduction of $HRu_3(CO)_{10}(NO)$ under H_2 was studied under a variety of conditions and yielded the products shown in eq 3. Table II shows the yields of the

$$HRu_3(CO)_{10}(NO) + H_2 \rightarrow H_4Ru_4(CO)_{12} + HRu_3(NH_2)(CO)_{10} + H_2Ru_3(NH)(CO)_9 + H_3Ru_4(NH_2)(CO)_{12} + \text{unknown} \quad (3)$$

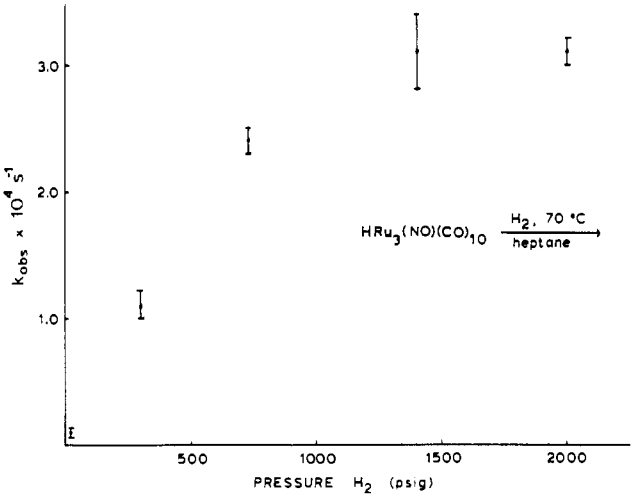

Figure 3. Graph illustrating the dependence of the observed rate of $HRu_3(CO)_{10}(NO)$ disappearance as a function of the pressure of hydrogen.

hexane-soluble products for a variety of reaction conditions. The characterization of each of these clusters will be discussed below. The unknown, which is soluble in THF and CH_2Cl_2, is insoluble in hexane and forms as a precipitate during the reaction. In THF it exhibits ν_{CO} absorbances in the terminal CO region, and the ^1H NMR spectrum exhibits several peaks in the metal hydride region from −16 to −21 ppm. A complete elemental analysis corresponded to the formula $C_9H_9NO_9Ru_2$. Unfortunately, all attempts to crystallize this compound (or separate the mixture) were unsuccessful.

The actual yields of the individual products were dependent on the reaction conditions. The variables studied were temperature, time, hydrogen pressure, and carbon monoxide pressure. Below 60 °C the reaction was too slow to observe regardless of the H_2 pressure. Above 90 °C the products as well as the starting material decompose. The effect of time on the reaction is best illustrated in Figure 2, which shows the product distribution as a function of time. Several important points are highlighted from this figure. First, the sequence of appearance of products containing N–H bonds is $H_2Ru_3(NH)(CO)_9$ *followed by* $HRu_3(NH_2)(CO)_{10}$. Second, at any one time during the reaction the total concentration of hexane-soluble N–H-containing products never exceeds 40% of the quantity of $HRu_3(CO)_{10}(NO)$ reacted. The mass balance in ruthenium is made up by the insoluble unknown and $H_4Ru_4(CO)_{12}$, which is only slightly soluble in hexane under these conditions. The third feature of the reduction is that the rate of disappearance of $HRu_3(CO)_{10}(NO)$ follows first-order kinetics for 2 half-lives. The observed rate constant at 75 °C and 2000 psig of H_2 was $(3.1 \pm 0.1) \times 10^{-4}\ s^{-1}$. When CO was added to the reaction mixture, the rate was slowed. For instance, with a mixture of 1500 psig of H_2 and 500 psig of CO at 75 °C no reaction was observed after 14 h.

The reaction rate was also dependent on the H_2 pressure. As shown in Figure 3, the rate steadily increases between 0 and 1400 psig, where it reaches a limit. The rate of stirring is not the cause of the saturation effect. These data (CO inhibition and H_2 saturation) suggest that reversible CO loss followed by oxidative addition of hydrogen (eq 4 and 5) are the first two steps of the reaction.

$$HRu_3(CO)_{10}(NO) \underset{k_{-1}}{\overset{k_1}{\rightleftharpoons}} CO + HRu_3(CO)_9(NO) \quad (4)$$

$$HRu_3(CO)_9(NO) + H_2 \xrightarrow{k_2} H_3Ru_3(CO)_9(NO) \quad (5)$$

$Ru_3(NOCH_3)(CO)_{10} + H_2$. $Ru_3(NOCH_3)(CO)_{10}$ reacts with H_2 under mild conditions (35 psig, 60 °C, 5 h) to lose CO and form $H_2Ru_3(NOCH_3)(CO)_9$ (eq 6). Under 1550 psig of H_2 and

$$Ru_3(NOCH_3)(CO)_{10} + H_2 \rightarrow CO + H_2Ru_3(NOCH_3)(CO)_9 \quad (6)$$

350 psig of CO the rate of this reaction is decreased. Under high-pressure conditions at 75 °C eq 6 proceeds rapidly and is followed by further reduction to $H_2Ru_3(NH)(CO)_9$ and $HRu_3(NH_2)(CO)_{10}$. With use of ^1H NMR spectroscopy the oxygen-containing product was identified as methanol. In this reduction no precipitate is formed during the reaction and the recovery of hexane-soluble ruthenium products is correspondingly higher. Equation 7 describes the overall process. The rate of conversion

$$Ru_3(NOCH_3)(CO)_{10} \xrightarrow{H_2} H_2Ru_3(NOCH_3)(CO)_9 \xrightarrow{H_2} H_2Ru_3(NH)(CO)_9 + HRu_3(NH_2)(CO)_{10} + H_4Ru_4(CO)_{12} + CH_3OH \quad (7)$$

of $H_2Ru_3(NOCH_3)(CO)_9$ to products shows a H_2 saturation effect similar to that found for $HRu_3(CO)_{10}(NO)$. The maximum rate, $(4.6 \pm 1.0) \times 10^{-5}$ s^{-1}, was obtained at 900 psig of H_2. Also found was that CO strongly inhibits the rate of $H_2Ru_3(NOCH_3)(CO)_9$ reaction.

$Ru_3(NOH)(CO)_{10} + H_2$. In the region of 15–2000 psig of H_2, $Ru_3(NOH)(CO)_{10}$ led mostly to a hexane-insoluble product and very small amounts of $HRu_3(NH_2)(CO)_{10}$, $H_2Ru_3(NH)(CO)_9$, $HRu_3(CO)_{10}(NO)$, and $H_4Ru_4(CO)_{12}$. As in the reduction of $HRu_3(CO)_{10}(NO)$ the hexane-insoluble product found here is soluble in THF and CH_2Cl_2. The infrared spectrum exhibits a very strong peak at 2040 cm^{-1} with a shoulder at 2000 cm^{-1} and a weak peak at 2110 cm^{-1}. This is very similar to the spectrum obtained from the hexane-insoluble material resulting from the reduction of $HRu_3(CO)_{10}(NO)$.

Characterization of the Products. Table I shows the spectroscopic data for each of the clusters discussed in this paper. The experimental section contains the data supporting the formulation of these clusters.

The compounds having the formula $H_2Ru_3(NR)(CO)_9$ with R = H,[14] OCH_3[11] have infrared spectra that are similar to one another as well as to those of the structurally characterized compounds $H_2Ru_3(NPh)(CO)_9$[20] (I), $H_2Ru_3S(CO)_9$,[21] $H_2Os_3(NPh)(CO)_9$,[22] and $H_2Os_3(NCH_3)(CO)_9$.[23] In each case we assigned the structure of the clusters to contain a μ_3-NH (II) or a μ_3-$NOCH_3$ (III). For the clusters with a μ_3-NH both ν_{N-H} and $\delta(^1H)$ show a strong dependence on the metal. For $H_2Ru_3(NH)(CO)_9$ the value of the N–H stretch is 3362 cm^{-1}, which is similar to that of other clusters such as $FeCo_2(NH)(CO)_9$ (3357 cm^{-1})[14] and $Fe_3(NH)(CO)_{10}$ (3368 cm^{-1}).[24] The osmium clusters $H_2Os_3(NH)(CO)_9$ and $H_4Os_3(NH)(CO)_8$ both have N–H stretching frequencies about 20 cm^{-1} higher in energy at 3382 and 3390 cm^{-1}, respectively.[25] There is a notable dependence of the chemical shift of the imido hydrogen on the metals as seen in the following series: $FeCo_2(NH)(CO)_9$, 10.62 ppm;[14] $Fe_3(NH)(CO)_{10}$,[24] 9.50 ppm; $H_2Ru_3(NH)(CO)_9$, 6.36 ppm; $H_4Os_3(NH)(CO)_8$, 4.42 ppm; $H_2Os_3(NH)(CO)_9$, 4.06 ppm.[25] Between $H_2Ru_3(NH)(CO)_9$ and $H_2Os_3(NH)(CO)_9$ there is also a 2 ppm upfield shift in the position of the metal hydrides that matches the 2.3 ppm shift in the imido hydrogen. The ^{15}N NMR spectrum of $H_2Ru_3(NH)(CO)_9$ exhibits an absorbance at 82.5 ppm downfield from liquid NH_3. $J_{^{15}N-^1H} = 77.5$ Hz, which is characteristic of a direct N–H bond. When the hydrogen (of the N–H) is replaced with $-OCH_3$, the ^{15}N chemical shift drops to 301.0 ppm.

The cluster having the formulation $HRu_3(NH_2)(CO)_{10}$ is a new member of a very common class of trinuclear ruthenium clusters having one edge of the triangle bridged by a hydrogen and a three-electron donor.[26] Many of these compounds have been structurally characterized, and they exhibit a characteristic pattern in the carbonyl stretching region of the infrared spectrum. $HRu_3(NH_2)(CO)_{10}$ also exhibits this pattern (Table I), and the structure (IV) was verified by a single-crystal X-ray crystallographic study described below. In the ^{15}N NMR spectrum of $HRu_3(NH_2)(CO)_{10}$, the resonance is centered at −33.5 ppm relative to ammonia, and it exhibits coupling to all three hydrogen atoms in the molecule. The directly bound N–H couplings are 72.7 and 70.9 Hz, and the two-bond coupling to the hydride ligand is 2.5 Hz.

In larger scale reductions of $HRu_3(CO)_{10}(NO)$ trace amounts of a compound tentatively identified as $H_3Ru_4(NH_2)(CO)_{12}$ were isolated. The formulation is analogous to three structurally characterized clusters: $H_3Ru_4(NCO)(CO)_{12}$,[27] $H_3Os_4(CO)_{12}(NO)$,[28] and $H_3Os_4(I)(CO)_{12}$.[29] The similarity in the infrared and ^1H NMR spectra with those of $H_3Ru_4(NCO)(CO)_{12}$ is the basis for its identification. As with the isocyanato cluster no parent ion is observed in the mass spectrum, and we suggest that $H_3Ru_4(NH_2)(CO)_{12}$ has the structure shown in V. There is one

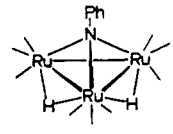

I

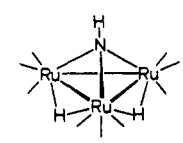

II

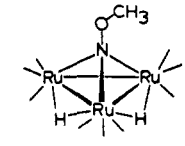

III

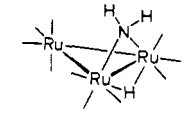

IV

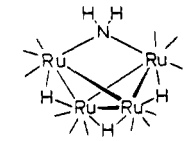

V

(20) Bhaduri, S.; Gopalkrishnan, K. S.; Clegg, W.; Jones, P. G.; Sheldrick, G. M.; Stalke, D. *J. Chem. Soc., Dalton Trans.* **1984**, 1765.
(21) Adams, R. D.; Katahira, D. A. *Organometallics* **1982**, *1*, 53.
(22) Burgess, K.; Johnson, B. F. G.; Lewis, J.; Raithby, P. R. *J. Organomet. Chem.* **1982**, *224*, C40.
(23) Lin, Y. C.; Knobler, C. B.; Kaesz, H. D. *J. Organomet. Chem.* **1981**, *213*, C41.
(24) Fjare, D. E.; Gladfelter, W. L. *Inorg. Chem.* **1981**, *20*, 3533.
(25) Smieja, J. A.; Gladfelter, W. L. *J. Organomet. Chem.*, in press.
(26) Bruce, M. I. In "Comprehensive Organometallic Chemistry: The Synthesis, Reactions and Structures of Organometallic Compounds"; Wilkinson, G., Ed.; Pergamon Press: Oxford, England, 1982; Vol. 4, p 843.
(27) Fjare, D. E.; Jensen, J. A.; Gladfelter, W. L. *Inorg. Chem.* **1983**, *22*, 1774.
(28) Braga, D.; Johnson, B. F. G.; Lewis, J.; Mace, J. M.; McPartlin, M.; Nelson, W. J. H.; Puga, J.; Raithby, P. R.; Whitmire, K. H. *J. Chem. Soc., Chem. Commun.* **1982**, 1081.
(29) Johnson, B. F. G.; Lewis, J.; Raithby, P. R.; Wong, K.; Rouse, K. D. *J. Chem. Soc., Dalton Trans.* **1980**, 1248.

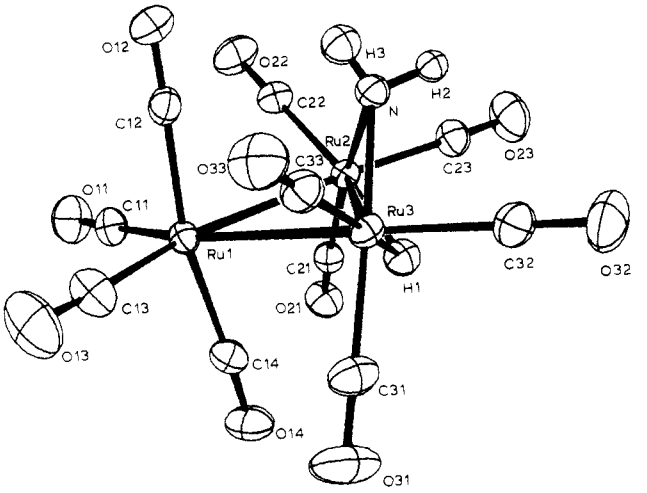

Figure 4. View of $HRu_3(NH_2)(CO)_{10}$ showing the atom labels.

interesting spectral difference between the bridging NH_2 in this tetranuclear cluster and that in $HRu_3(NH_2)(CO)_{10}$. Both the symmetric and asymmetric N–H stretches are approximately 35 cm^{-1} lower in energy in $H_3Ru_4(NH_2)(CO)_{12}$, and the hydrogen (of the NH_2) chemical shift is 3 ppm upfield (at −1.08 ppm) relative to $HRu_3(NH_2)(CO)_{10}$.

X-ray Structural Analysis of $HRu_3(NH_2)(CO)_{10}$. Figure 4 shows a view of the structure with the atomic labeling scheme. Tables V and VI contain the distances and selected bond angles for $HRu_3(NH_2)(CO)_{10}$. The structure consists of an isosceles triangle of Ru atoms with one edge bridged by both a NH_2 and a H atom. This edge (Ru2–Ru3) is 0.06 Å shorter than the average of the other two edges. Each of the ten carbonyl ligands is coordinated to the metals in a linear, terminal fashion. The M–C bond distances range from 1.896 (Ru3–C33) to 1.941 Å (Ru1–C14). In other studies of $HRu_3(\mu\text{-}X)(CO)_{10}$ structures the M–C bond distance of the CO ligand trans to the μ-X ligand has depended on the nature of X.[26] Typically, strong ligands bound to the metal via carbon as in $HRu_3(COMe)(CO)_{10}$ cause a lengthening of the trans-M–CO bond while X groups bound via heteroatoms cause little or no lengthening. This cluster with a bridging NH_2 also fits this pattern.

The amido ligand symmetrically bridges Ru2 and Ru3, having Ru–N distances of 2.102 (2) and 2.101 (2) Å, respectively. The Ru2–N–Ru3 angle is 82.47 (8)°, which is comparable to that found in $HRu_3(NCH_2Ph)(CO)_{10}$.[30] The hydrogen atoms were located, but the accuracy of the positions is not high. The H2–N–H3 angle is 100 (3)°, and the N–H2/3 distances are 0.88 (3) and 0.79 (4) Å. These values are similar to those found in other bridging NH_2 ligands. One final noteworthy point is the intermolecular H bonding between H2 and O33. The N–H2···O33 interaction is linear, and the O33···H2 distance is 2.44 (3) Å.

Conversions of μ_3-NR Ligands to μ-NHR Ligands. In this study we have examined several reactions involving the formation of an N–H bond concurrent with the conversion of a triply bridging ligand to an edge-bridging ligand. The reaction for $H_2Ru_3(NH)(CO)_9$ (eq 8) occurred more readily than any of the other

$$H_2Ru_3(NH)(CO)_9 + CO \xrightarrow[1.5\ h]{95\ °C,\ 50\ psig} HRu_3(NH_2)(CO)_{10} \quad 54\%\ yield \tag{8}$$

conversions. Even under a nitrogen atmosphere pyrolysis of $H_2Ru_3(NH)(CO)_9$ was found to yield some $HRu_3(NH_2)(CO)_{10}$. We attempted to reverse this reaction under a variety of conditions, yet $H_2Ru_3(NH)(CO)_9$ was never formed from $HRu_3(NH_2)(CO)_{10}$. Even in refluxing decalin (~160 °C) under nitrogen for 5 h no $H_2Ru_3(NH)(CO)_9$ formed, even though the $HRu_3(NH_2)(CO)_{10}$ had completely disappeared. The major hexane-soluble species was $H_4Ru_4(CO)_{12}$. Similar results were found at lower temperatures.

In order to evaluate this reaction with other μ_3-NR groups, we prepared the known cluster $H_2Ru_3(NPh)(CO)_9$.[12] Under 50 psig of CO at temperatures ranging from 95 to 110 °C slow conversion to $HRu_3(NHPh)(CO)_{10}$ and $Ru_3(NPh)(CO)_{10}$ was observed. After 22 h of heating only 40% of the starting material had reacted, and the two products $HRu_3(NHPh)(CO)_{10}$ and $Ru_3(NPh)(CO)_{10}$ were formed in a 3:1 ratio, respectively.

The final ruthenium cluster tested was $H_2Ru_3(NOCH_3)(CO)_9$, and it was also very slow to react. When it did react, the only characterized products that were isolated (in very low yield) no longer contained the $NOCH_3$ ligand. Species containing the NCO ligand and trace amounts of $H_2Ru_3(NH)(CO)_9$, $HRu_3(NH_2)(CO)_{10}$, and $Ru_3(CO)_{12}$ were formed.

Discussion

Mechanistic Aspects of the Reduction of Coordinated Nitric Oxide with Molecular Hydrogen. A detailed account of the NO reduction in $HRu_3(CO)_{10}(NO)$ must necessarily involve a large number of steps. Of particular interest are those that directly involve the NO ligand. From NO to NH the following four primary steps must occur in some order: (1) N–O bond cleavage, (2) N–H bond formation, (3) the first O–H bond formation (assuming H_2O is the product), and (4) the second O–H bond formation. Interspersed among these reactions the activation of 2 mol of molecular hydrogen must also occur. Clearly, the overall complexity is too great to allow a single mechanism to be proven with our current data. Our studies do allow us to comment on several aspects of this reaction and ultimately to propose a reasonable scenario that can account for the observed products.

Cleavage of the N–O bond is the central issue in understanding this mechanism. The oxygenated product is presumably H_2O, but we have not unambiguously proven this. The similarity in reaction products between the reductions of $HRu_3(CO)_{10}(NO)$ and $H_2Ru_3(NOCH_3)(CO)_9$, in which CH_3OH is eliminated, is a strong case supporting H_2O loss. In the reduction of $HRu_3(CO)_{10}(NO)$ this would mean that the first O–H bond would form (giving an NOH ligand) prior to N–O bond cleavage. The literature contains two examples of clusters containing the N–O–H ligand. In both $Ru_3(NOH)(CO)_{10}$[11] and $[(C_5H_4Me)_3Mn_3(NO)_3(NOH)]^{+}$[6] the NOH is triply bridging a triangle of metals. The former cluster is particularly relevant, since it is the tautomer of the starting nitrosyl complex, $HRu_3(CO)_{10}(NO)$, in this work.

The kinetic analysis of the disappearance of $HRu_3(CO)_{10}(NO)$ allows the definition of the first two steps in the mechanism: reversible CO dissociation followed by H_2 oxidative addition. Scheme I shows possible structures for $HRu_3(CO)_9(NO)$ and $H_3Ru_3(CO)_9(NO)$. The mechanistic steps proposed here match those found by Keister and co-workers for the hydrogenation of the isostructural and isoelectronic cluster $HRu_3(COMe)(CO)_{10}$.[31] In their further kinetic studies the importance of the μ_3-η^2-COMe ligand in stabilizing the unsaturated intermediate has been suggested.[32] With the additional hydrogen atoms available and the possible presence of μ_3-NO, tautomerization may become favorable. This shift of the hydrogen from the metal to the oxygen has a precedent from the studies of Andrews and Kaesz,[33] where the μ_3-η^2-N=CR_2 ligand, which is isoelectronic with μ-NO, was converted into the μ_3-N—CHR_2 ligand on a triiron cluster (eq 9). Recent studies reported similar reactions with triruthenium

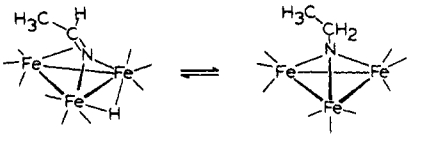

(9)

(30) Lausarot, P. M.; Vaglio, G. A.; Valle, M.; Tiripicchio, A.; Camellini, M. A. *J. Chem. Soc., Chem. Commun.* **1983**, 1391.

(31) Bavaro, L. M.; Montangero, P.; Keister, J. B. *J. Am. Chem. Soc.* **1983**, *105*, 4977.

(32) Dalton, D. M.; Barnett, D. J.; Duggan, T. P.; Keister, J. B.; Malik, P. T.; Modi, S.; Shaffer, M. R.; Smesko, S. A., manuscript in preparation. We are grateful to J. B. Keister for early communication of these results.

(33) Andrews, M. A.; Kaesz, H. D. *J. Am. Chem. Soc.* **1979**, *101*, 7255.

Scheme I

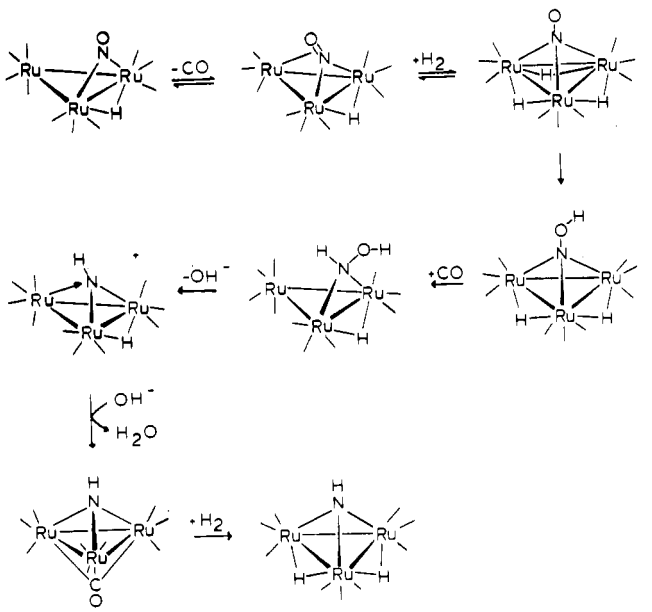

clusters.[34,35] The product of tautomerization of $H_3Ru_3(CO)_9(NO)$ would be $H_2Ru_3(NOH)(CO)_9$. Although we have not been able to isolate $H_2Ru_3(NOH)(CO)_9$ from the hydrogenation of $HRu_3(CO)_{10}(NO)$ or $Ru_3(NOH)(CO)_{10}$, we have obtained and characterized the $NOCH_3$ analogue, $H_2Ru_3(NOCH_3)(CO)_9$, from the reaction of $Ru_3(NOCH_3)(CO)_{10}$ with H_2.

The next proposed step in Scheme I is the conversion of the μ_3-NOH ligand to a μ-NHOH ligand. We have observed the identical reaction when the group attached to the nitrogen is –H and –Ph instead of –OH. For $H_2Ru_3(NH)(CO)_9$ the conversion to $HRu_3(NH_2)(CO)_{10}$ is facile with or even without added CO:

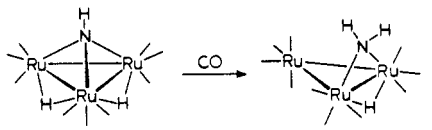

(10)

In the latter case the reaction occurs in lower yield. For $H_2Ru_3(NPh)(CO)_9$ the predominant product is $HRu_3(NHPh)(CO)_{10}$, however, some $Ru_3(NPh)(CO)_{10}$ is also formed. This reaction is notably slower than for the μ_3-NH cluster and as such provides an interesting substituent effect. The reaction itself is of some importance since it represents a rare example of the first step in the removal of a triply bridging ligand from an intact metal cluster. It can be viewed as the reductive elimination of an N–H bond, leaving a vacant site for CO to add. Alternatively under high pressures of H_2, activation of molecular hydrogen could occur to give $H_3Ru_3(NHR)(CO)_9$. While this would affect the formulas of the subsequent steps in Scheme I, the same steps would still lead to $H_2Ru_3(NH)(CO)_9$ as the first product. In other words, H_2 must be added to the cluster a second time (the first time occurs in the formation of $H_3Ru_3(CO)_9(NO)$), and we cannot state at what point in the mechanism this occurs. We attempted to convert $H_2Ru_3(NOCH_3)(CO)_9$ into $HRu_3(NHOCH_3)(CO)_{10}$ but found no such species. The only isolable product was small amounts of $HRu_3(NH_2)(CO)_{10}$. The intermediacy of the hydroxyimido ligand (NHOH) was also proposed by Johnson, Lewis, and Mace in their studies of this system.[9]

With $HRu_3(NHOH)(CO)_{10}$ we believe the stage is now set for cleavage of the N–O bond. We propose that simple heterolysis can occur to give OH^- and a cationic cluster formulated as $[HRu_3(NH)(CO)_{10}]^+$. The hydroxide could easily deprotonate the cluster to give $Ru_3(NH)(CO)_{10}$, which we have independently prepared.[36] We have found that this cluster, $Ru_3(NH)(CO)_{10}$, reacts readily with hydrogen to form $H_2Ru_3(NH)(CO)_9$. The cationic cluster $[HRu_3(NH)(CO)_{10}]^+$ is isoelectronic with the structurally characterized osmium trimer $HOs_3(CH)(CO)_{10}$, recently prepared by Shapley and co-workers.[37] As shown in eq 11 even the method of preparation of $HOs_3(CH)(CO)_{10}$ provides precedent for the N–O cleavage step in Scheme I.

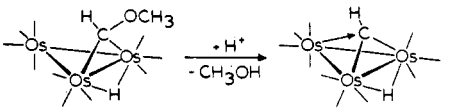

(11)

The involvement of highly acidic species such as a μ_3-NOH ligand could easily be the reason a precipitate forms in hexane. Consistent with this, when we started with pure $Ru_3(NOH)(CO)_{10}$ the major product was the hexane-insoluble compound, and the amount formed was far greater than the amount formed when $HRu_3(CO)_{10}(NO)$ was used. By infrared spectroscopy the hexane-insoluble products formed from $HRu_3(CO)_{10}(NO)$ and $Ru_3(NOH)(CO)_{10}$ are the same species. Further support for this idea comes from the study of $Ru_3(NOCH_3)(CO)_{10}$, which, having no ionizable hydrogens, reduces with H_2 to give the same products but no precipitate.

The other major product found in this reaction is $H_4Ru_4(CO)_{12}$. This compound represents a thermodynamic sink whenever mixtures of H_2 and ruthenium carbonyls are formed[13] and represents the end point of the reaction under the conditions studied. While the source of some of this compound was shown to result from further reaction of $HRu_3(NH_2)(CO)_{10}$ with H_2, presumably with elimination of NH_3, not all of the material can originate from here. It is reasonable to expect that some of the intermediates can add H_2 and continue directly on to $H_4Ru_4(CO)_{12}$. The tetranuclear cluster $H_3Ru_4(NH_2)(CO)_{12}$, which is found only in the larger scale reactions, could be the immediate precursor to ammonia dissociation via the steps shown in eq 12.

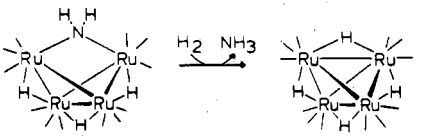

(12)

Unambiguous proof that NH_3 is the ultimate nitrogenous product has not yet been obtained. In the related compound $H_2Ru_3(NPh)(CO)_9$, Bhaduri and co-workers found that aniline is released under 150 psig of CO at 30 °C.[20] Apparently, in our experiments conducted at 50 psig of CO and 100 °C, formation of the intermediate $HRu_3(NHPh)(CO)_{10}$ is found. Further studies in progress are examining the several N–H bond-forming steps, including the last step in the reaction.

Acknowledgment. We wish to thank the National Science Foundation for supporting this research (Grant No. CHE-8410999).

Registry No. $HRu_3(CO)_{10}(NO)$, 73230-19-0; $Ru_3(NOH)(CO)_{10}$, 83333-40-8; $Ru_3(NOCH_3)(CO)_{10}$, 83333-39-5; $H_4Ru_4(CO)_{12}$, 34438-91-0; $H_2Ru_3(NH)(CO)_9$, 86743-32-0; $HRu_3(NH_2)(CO)_{10}$, 90424-85-4; $H_3Ru_4(NH_2)(CO)_{12}$, 97633-47-1; $Ru_3(CO)_{12}$, 15243-33-1; $H_2Ru_3(NOCH_3)(CO)_9$, 83312-29-2; $H_2Ru_3(NPh)(CO)_9$, 51185-97-8; $HRu(NHPh)(CO)_{10}$, 51186-00-6; $Ru_3(NPh)(CO)_{10}$, 51185-99-0; H_2, 1333-74-0; NO, 10102-43-9; H_2NOH, 7803-49-8; H_2NOCH_3, 67-62-9.

Supplementary Material Available: Listings of calculated and observed structure factors, atomic coordinates and thermal parameters, and general temperature factors and a complete listing of bond distances and angles (30 pages). Ordering information is given on any current masthead page.

(34) Bernhardt, W.; Vahrenkamp, H. *Angew. Chem., Int. Ed. Engl.* **1984**, *23*, 381.

(35) Lausarot, P. M.; Turini, M.; Vaglio, G. A.; Valle, M.; Tiripicchio, A.; Tiripicchio Camellini, m.; Gariboldi, P. *J. Organomet. Chem.* **1984**, *273*, 239.

(36) Blohm, M. L.; Fjare, D. E.; Gladfelter, W. L., submitted for publication.

(37) Shapley, J. R.; Cree-Uchiyama, M. E.; St George, G. M.; Churchill, M. R.; Bueno, C. *J. Am. Chem. Soc.* **1983**, *105*, 140.